Journal of Alloys and Compounds 509 (2011) 5655–5659

Contents lists available at ScienceDirect

Journal of Alloys and Compounds

journal homepage: www.elsevier.com/locate/jallcom

Luminescent properties of $Na_3Gd_{1-x}Eu_x(PO_4)_2$ and energy transfer in these phosphors

Guifang Ju, Yihua Hu*, Li Chen, Xiaojuan Wang, Zhongfei Mu, Haoyi Wu, Fengwen Kang

School of Physics and Optoelectronic Engineering, Guangdong University of Technology, Waihuan Xi Road, No. 100, Guangzhou 510006, Guangdong, People's Republic of China

ARTICLE INFO

Article history:
Received 1 January 2011
Received in revised form 17 February 2011
Accepted 19 February 2011
Available online 26 February 2011

Keywords:
Phosphors
Solid state reaction
Optical properties
Luminescent property

ABSTRACT

A series of Eu^{3+} activated $Na_3Gd_{1-x}Eu_x(PO_4)_2$ ($0 \le x \le 1$) phosphors were synthesized by solid-state reaction method. The structures and photo-luminescent properties of these phosphors were investigated at room temperature. The results of XRD patterns indicate that these phosphors are isotypic to the orthorhombic $Na_3Gd(PO_4)_2$. The excitation spectra indicate that these phosphors can be effectively excited by near UV (370–410 nm) light. The intensities of magnetic dipole transition $^5D_0 \rightarrow {}^7F_1$ and forced electric dipole transition $^5D_0 \rightarrow {}^7F_2$ are comparable, and the energy ratio ($^5D_0 \rightarrow {}^7F_1/{}^5D_0 \rightarrow {}^7F_2$) is 1.1. The emission spectra exhibit strong reddish orange performance (CIE chromaticity coordinates: $x = 0.62$, $y = 0.38$), which is due to the $^5D_0 \rightarrow {}^7F_J$ transitions of Eu^{3+} ions. The correlation between the structure and the photo-luminescent properties of the phosphors was studied. The energy transfer and concentration quenching of the phosphors were discussed. $Na_3Gd_{1-x}Eu_x(PO_4)_2$ has a potential application for white light-emitting diodes.

1. Introduction

The white light-emitting diode (WLED) has attracted increasing attention as a new light source for illumination and displays with its high efficiency, long lifetime and mercury free [1–6]. There are several approaches to generate WLEDs. Today, the WLED market is dominated by phosphor-converted WLEDs normally comprising a 450–470 nm blue InGaN LED chip covered by a yellow phosphor, which is usually made of YAG:Ce^{3+} [7–12]. However, phosphor-converted WLEDs made by means of blue-LED + yellow phosphor suffer from the drawbacks such as halo effect due to the different emission characteristics of the LEDs (directional) and the phosphors (isotropic) [13], low color rendering index (CRI) and high color temperature caused by lack of red component in the spectra [2,7,10–12,14,15]. White light can also be produced by another method, i.e., using a near ultraviolet (NUV) LED (370–410 nm) to stimulate the mixture of red, green and blue (RGB) phosphors [1–3,7,10]. NUV LEDs with RGB phosphor mixtures provide a better CRI value, and therefore, are suitable for indoor applications. However, oxide phosphors (in particular, red phosphors) with excitation spectra matching the NUV excitation are rare, whereas sulfide (or oxysulfide) and nitride (or oxynitride) phosphors suffer from stability and synthesis problems, respectively [16]. Therefore, there is an urgent need to produce red-emitting phosphors which can be efficiently excited by NUV light. In this work, we choose Eu^{3+} ions as activators since they may have strong absorption bands at 370–410 nm ($^7F_0 \rightarrow {}^5L_{6,7}, {}^5G_J$). Moreover, they exhibit a high lumen equivalent, quantum efficiency and stability at the same time.

Unfortunately, in Russell–Saunders coupling electric dipole (ED) transitions within the 4f configuration are weak (spin and parity forbidden), even though selection rules are partly lifted by spin–orbit interaction and crystal field [17]. Hence, Eu^{3+} activated red phosphors for WLEDs should be heavily doped or stoichiometric to enhance absorption. Owing to its unique energy level scheme, profound concentration quenching can be suppressed in suitable matrix. In the present work, $Na_3Gd(PO_4)_2$ was adopted.

The polycrystalline $Na_3Gd(PO_4)_2$ belongs to the orthorhombic system with space group Pcmb (Number = 57, $Z = 8$) [18,19]. The structural and spectroscopic properties of the alkali metal lanthanide double phosphates, $M_3R(PO_4)_2$ (R = trivalent lanthanide ions), doped with different lanthanide ions have been subject to considerable interest in the past [19–36]. However, there are no detailed reports on the photo-luminescent properties of $Na_3Gd(PO_4)_2$:Eu^{3+} under NUV excitation, i.e., little research on potential application in phosphor-converted WLEDs has been report. The main purpose of this work is to directly investigate the spectroscopic properties of $Na_3Gd(PO_4)_2$:Eu^{3+} under NUV excitation and possible applications.

2. Experimental

2.1. Synthesis

The powder samples of $Na_3Gd_{1-x}Eu_x(PO_4)_2$ ($0 \le x \le 1$) were prepared by solid-state reaction technique at high temperature. The starting materials were Na_2CO_3

* Corresponding author. Tel.: +86 020 39322262; fax: ++86 020 39322265.
E-mail address: huyh@gdut.edu.cn (Y. Hu).

0925-8388/$ – see front matter © 2011 Elsevier B.V. All rights reserved.
doi:10.1016/j.jallcom.2011.02.110

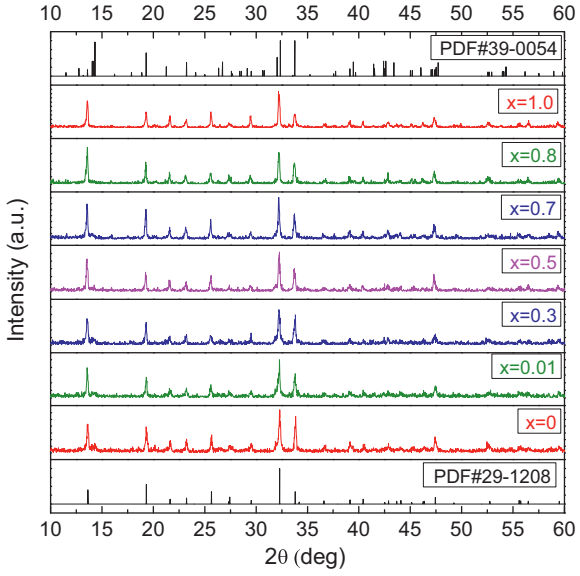

Fig. 1. The XRD patterns of the samples.

(A.R.), $(NH_4)_2HPO_4$ (A.R.), Gd_2O_3 (4N), Eu_2O_3 (4N) and ethanol (A.R.). All raw materials with stoichiometric amounts were mixed homogeneously with small amounts of ethanol (to help grinding) in an agate mortar. The homogeneous mixture was put into a corundum crucible and calcined in a muffle furnace. The samples were heated from room temperature to 1000 °C at the rate of ~6 °C/min, after the 5 h calcinations at 1000 °C in air, the muffle furnace was turned off to cool down the samples.

2.2. Measurement

The phase purity of the prepared phosphors was checked by an X-ray diffractometer with Cu Kα radiation (wavelength = 0.15406 nm) at 36 kV tube voltage and 20 mA tube current. The excitation and emission spectra of all the samples were measured by a Hitachi F-7000 Fluorescence Spectrophotometer at room temperature.

3. Results and discussion

3.1. XRD phase analysis

The X-ray powder diffraction (XRD) patterns of $Na_3Gd_{1-x}Eu_x(PO_4)_2$ (x = 0, 0.01, 0.3, 0.5, 0.7, 0.8, 1.0) are shown in Fig. 1. The analysis of XRD patterns confirms that the compounds with higher x are consistent with the standard PDF#29-1208, which suggests $Na_3Gd_{1-x}Eu_x(PO_4)_2$ orthophosphates are isotypic to orthorhombic $Na_3Gd(PO_4)_2$. Some additional weak diffraction peaks are observed in the x < 0.7 samples at 14–14.4°, they are indexed as the monoclinic $Na_3Gd(PO_4)_2$ (PDF#39-0054). The double phosphates $Na_3R(PO_4)_2$ containing lanthanides from La to Sm crystallize only in the low temperature orthorhombic phase, while all the lanthanides between Gd and Er crystallize in the high temperature orthorhombic form and then monoclinic form [24]. Therefore it is not easy to get pure orthorhombic $Na_3Gd_{1-x}Eu_x(PO_4)_2$ when x is small. The impurity peaks are very weak, so profound influence on spectroscopic results is not expected. As we mentioned in the introduction section, Eu^{3+} activated red phosphors for WLEDs should be heavily doped, so the impurity in lower x samples is not a problem. The radius of Eu^{3+} ion (~106.6 pm) is similar to that of Gd^{3+} ion (~105.3 pm) with coordination number eight [37]; therefore, Eu^{3+} and Gd^{3+} can form a continuous solid solution in the matrix. The cell parameters are calculated and shown in Fig. 2. With the increase of the Eu^{3+} concentration (x), the cell constants and cell volumes slightly increase due to the substitution of Gd^{3+}. The R^{3+} ions are connected through O–P–O linkages in this compound and

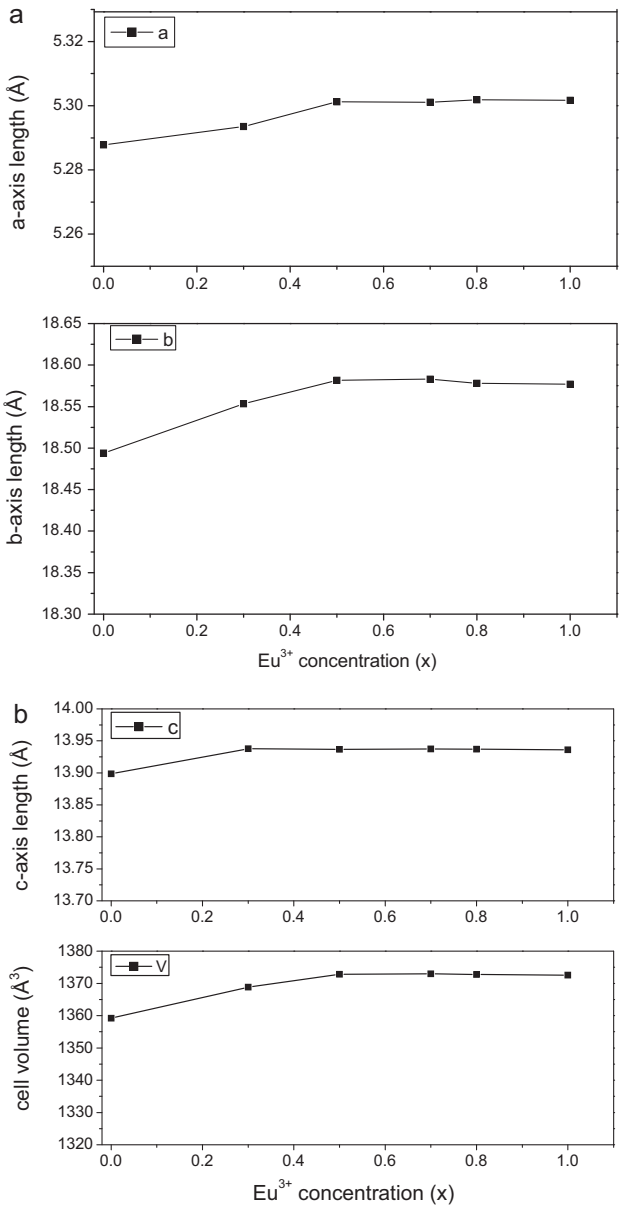

Fig. 2. The calculated cell parameters of $Na_3Gd_{1-x}Eu_x(PO_4)_2$.

there are six different R^{3+} sites with two six-fold, three seven-fold and one eight-fold coordination to oxygen ions [19,24]. The positions for the R^{3+} give C_1 as the site symmetry for all the sites [24,35].

3.2. Photoluminescent properties of Eu^{3+} in $Na_3Gd_{1-x}Eu_x(PO_4)_2$

Fig. 3 gives the excitation spectra by monitoring the $^5D_0 \rightarrow {}^7F_{1,\ 2}$ emission (λ_{em} = 594 and 618 nm) of Eu^{3+} in the $Na_3Gd_{0.05}Eu_{0.95}(PO_4)_2$ phosphor and the excitation spectrum of $Na_3Gd_{0.99}Eu_{0.01}(PO_4)_2$ by monitoring the $^5D_0 \rightarrow {}^7F_1$ emission (λ_{em} = 594 nm). The spectra consist of a broad band and some sharp lines. The broad excitation band centered at ~250 nm can be attributed to the charge-transfer band (CTB) transition arising from O^{2-} ion to Eu^{3+} ion, at lower Eu^{3+} concentrations the CTB shifts to somewhat shorter wavelengths. The sharp lines of the $Na_3Gd_{0.05}Eu_{0.95}(PO_4)_2$ phosphor are ascribed to the intra-configurational 4f–4f transitions of Eu^{3+} in the host lattice: $^7F_0$ to $^5F_4$, $^5H_6$, $^5D_4$, ^5G_J, $^5L_7$, $^5L_6$, $^5D_3$, $^5D_2$ and $^5D_1$ at wavelengths

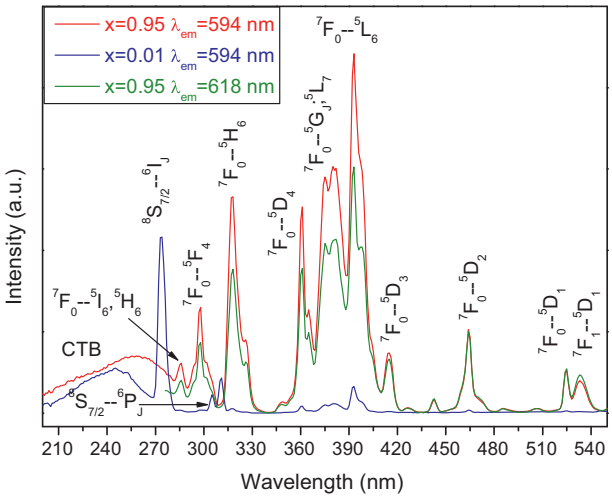

Fig. 3. The excitation spectra of $Na_3Gd_{1-x}Eu_x(PO_4)_2$ ($x = 0.01, 0.95$).

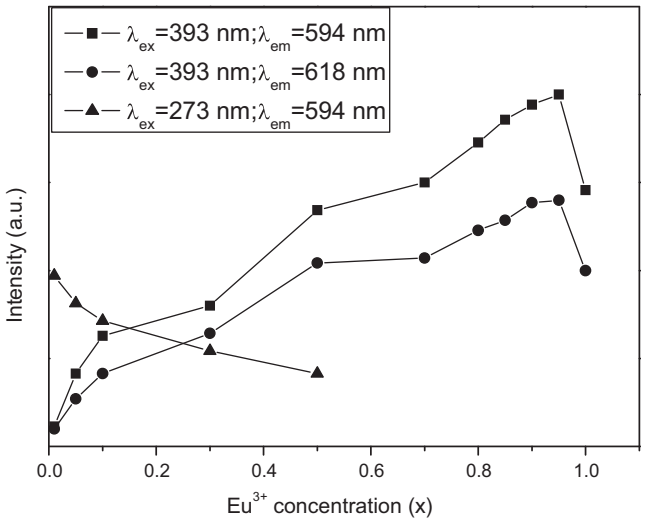

Fig. 5. The relative emission intensity of $Na_3Gd_{1-x}Eu_x(PO_4)_2$ varied with the concentration of Eu^{3+} (x).

298, 317, 361, 375, 380, 393, 415, 464 and 525 nm, respectively. At room temperature, the $^7F_1$ level is thermally populated due to the small energy gap of $^7F_1$ and $^7F_0$ (~370 cm^{-1}), so the transition of $^7F_1 \rightarrow {}^5D_1$ was observed at 533 nm. The strongest excitation bands are at 370–410 nm ($^7F_0 \rightarrow {}^5L_{6,7}$, ^5G_J). The obvious discrepancy between $Na_3Gd_{0.05}Eu_{0.95}(PO_4)_2$ and $Na_3Gd_{0.99}Eu_{0.01}(PO_4)_2$ in the spectra is that two more lines appear at ~273 and ~311 nm in the spectrum of $Na_3Gd_{0.99}Eu_{0.01}(PO_4)_2$, corresponding to the $^8S_{7/2} \rightarrow {}^6I_J$ and $^8S_{7/2} \rightarrow {}^6P_J$ transitions of Gd^{3+}, respectively. This implies that Gd^{3+} ion transfers its energy to Eu^{3+}; we will discuss it in the next section.

The Eu^{3+} activated compounds $Na_3Gd_{1-x}Eu_x(PO_4)_2$ show strong reddish orange emission under 393 or 273 nm excitation. The relative emission spectra of $Na_3Gd_{0.05}Eu_{0.95}(PO_4)_2$ ($\lambda_{ex} = 393$ and 375 nm) and $Na_3Gd_{0.99}Eu_{0.01}(PO_4)_2$ ($\lambda_{ex} = 273$ nm) are given in Fig. 4. The emission spectrum of $Na_3Gd_{0.05}Eu_{0.95}(PO_4)_2$ is comprised of groups of lines from the emission of Eu^{3+} intra-configurational 4f–4f transitions ($^5D_0 \rightarrow {}^7F_{0-4}$) at 580, 594, 618, 653 and 702 nm, respectively. The vibrational energy of PO_4 stretching modes is in the region 900–1500 cm^{-1} [20,22], therefore, no emission from higher Eu^{3+} excited levels was detected, even at $x = 0.01$, because of efficient multi-phonon relaxation in the phosphors. The emission spectra have complex structure at high resolution [20,26],

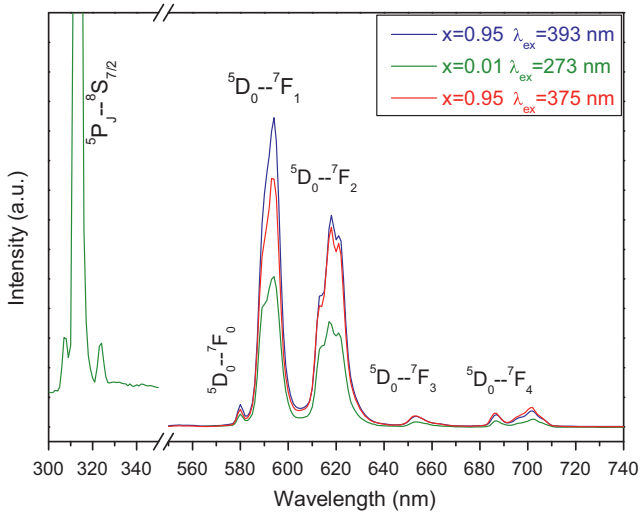

Fig. 4. The emission spectra of $Na_3Gd_{1-x}Eu_x(PO_4)_2$ ($x = 0.01, 0.95$).

due to the variety of Eu^{3+} sites and low site symmetry. But the low resolution spectra only show bold lines.

The forced ED transition $^5D_0 \rightarrow {}^7F_2$ with $\Delta J = 2$ is hypersensitive to local environment while the magnetic dipole (MD) transition $^5D_0 \rightarrow {}^7F_1$ with $\Delta J = 1$ is insensitive to the site symmetry, because it is parity-allowed. Hence, the MD/ED emission ratio can be used as a measure of the site symmetry of Eu^{3+} [see e.g., [38,39]]. The MD/ED ratio of $Na_3Gd_{1-x}Eu_x(PO_4)_2$ ($x > 0$) is 1.1, i.e., neither of the two transitions is dominant. Actually, the forced ED transition $^5D_0 \rightarrow {}^7F_2$ is also sensitive to the position of CTB. Intense forced ED emission from Eu^{3+} is expected only two conditions are fulfilled, viz. absence of inversion symmetry at the Eu^{3+} sites and lower CTB position [40]. The CTB of $Na_3Gd_{1-x}Eu_x(PO_4)_2$ locate at ~40,000 cm^{-1}, which is much higher than molybdates, tungstates and vanadates [2,40]. As we mentioned above, all rare-earth ions occupy crystallographic positions with C_1 point symmetry, which is not inversion symmetry center. The forced ED transition does not predominate in the emission spectra because only one condition is fulfilled.

The variation of emission intensities of $Na_3Gd_{1-x}Eu_x(PO_4)_2$ phosphors with Eu^{3+} concentration (x) are shown in Fig. 5. The most important feature of Fig. 5 is the fact that the quenching occurs above a Eu^{3+} concentration of 0.95, which indicates that below this concentration the excitation energy cannot migrate over the Eu^{3+} sublattice to killer sites. The electric multipole interactions between Eu^{3+} ions are weak due to the weak oscillator strength of $^7F_0 \leftrightarrow {}^5D_0$ [41], so only exchange interactions are of importance. However, The critical distance for exchange interactions between Eu^{3+} ions is 0.5 nm [42], while the minimum R–R distance in $Na_3Nd(PO_4)_2$ is equal to 0.465 nm [19], we suppose that in the case of $Na_3Gd_{1-x}Eu_x(PO_4)_2$ it is similar. Thus, energy migration over Eu^{3+} sublattice can take place, but it is not effective anyhow.

Fig. 6 presents the CIE 1931 color space chromaticity diagram to illustrate the chromaticity of $Na_3Gd_{1-x}Eu_x(PO_4)_2$ phosphors. The CIE coordinates of $Na_3Gd_{1-x}Eu_x(PO_4)_2$ ($x > 0$) were measured as $x = 0.62$, $y = 0.38$. Their corresponding location has been marked in Fig. 6 with a white cross. The CIE coordinates of $Na_3Gd_{1-x}Eu_x(PO_4)_2$ are in the reddish orange area (For interpretation of the references to colour in this figure text, the reader is referred to the web version of this article).

The emission spectrum of the sample $Na_3Gd_{0.99}Eu_{0.01}(PO_4)_2$ excited by 273 nm light due to $^8S_{7/2} \rightarrow {}^6I_J$ transitions within Gd^{3+} ion is comprised of both Eu^{3+} lines and Gd^{3+} lines, as shown in Fig. 4.

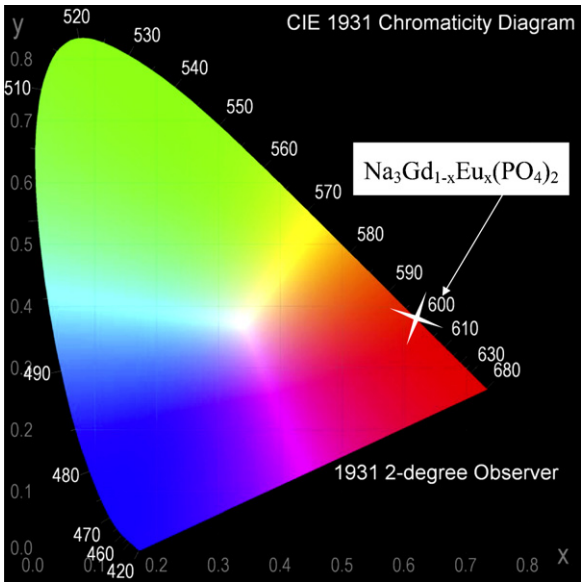

Fig. 6. CIE color space chromaticity diagram of $Na_3Gd_{1-x}Eu_x(PO_4)_2$ ($x>0$) phosphors.

The emission lines of Gd^{3+} ion at ~313 nm is due to the $^6P_{7/2} \rightarrow {}^8S_{7/2}$ transition.

3.3. Energy transfer from Gd^{3+} to Eu^{3+}

For excitation into the ^6I_J levels of Gd^{3+}, the emission curves of the phosphors co-doped with Gd^{3+} and Eu^{3+} ($x<0.2$) exhibit additional strong and narrow emission lines at 313 nm, accompanying the typical Eu^{3+} emission. It is evident that the energy which Gd^{3+} absorbed partly transfers to Eu^{3+}, and of course, this process comprising efficient energy migration in the Gd^{3+} sublattice, since the Eu^{3+} emission is strongest at lower Eu^{3+} concentration. For higher Eu^{3+} concentration, the emission of Gd^{3+} and Eu^{3+} is both quenched by the CTB (see Figs. 3, 5 and 7).

The energy transfer processes between activators are given in an energy level diagram, as shown in Fig. 7. Efficient energy transfer requires considerable energy overlap between donor emission band and accepter absorption band [42]. To discuss the $Gd^{3+} \rightarrow Eu^{3+}$ energy transfer we consider the relevant spectra Figs. 3 and 4. The Gd^{3+} emission lines ($^6P_{7/2} \rightarrow {}^8S_{7/2}$) overlap Eu^{3+} excitation lines

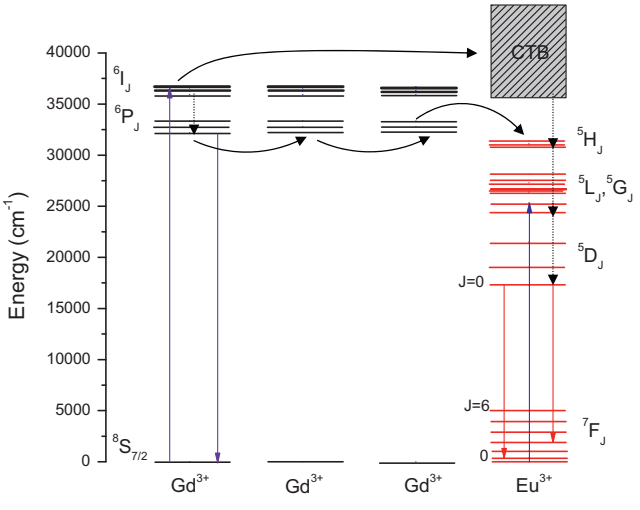

Fig. 7. Energy transfer scheme for $Na_3Gd_{1-x}Eu_x(PO_4)_2$.

($^7F_0 \rightarrow {}^5H_J$) at ~313 nm. Besides the energy overlap, efficient energy transfer also requires strong interactions, which may be electric multipole type or exchange type. As we mentioned at the previous section, the interaction between $Eu^{3+} \leftrightarrow Eu^{3+}$ is exchange mechanism, so it is reasonable that the exchange interaction may partly be responsible for the $Gd^{3+} \rightarrow Eu^{3+}$ energy transfer too, because there is no reason the wave function overlap vanishes in the $Gd^{3+} \rightarrow Eu^{3+}$ case. In contrast to $Eu^{3+} \leftrightarrow Eu^{3+}$ energy transfer, we can conclude that in the case of $Gd^{3+} \rightarrow Eu^{3+}$ there should be certain contribution of electric multipole interactions, because the oscillator strength of $^7F_0 \rightarrow {}^5H_J$ is much higher than $^7F_0 \rightarrow {}^5D_0$. The $Gd^{3+} \rightarrow Eu^{3+}$ energy transfer can also take place indirectly, as reported in $BaGdB_9O_{16}:Eu^{3+}$ [43], i.e., via the $O^{2-} \rightarrow Eu^{3+}$ CTB. Nevertheless, this indirectly energy transfer is not efficient anyway, because the CTB is much lower in contrast to $^7F_0 \rightarrow {}^5L_6$ line (Fig. 3).

4. Conclusions

Reddish orange phosphors $Na_3Gd_{1-x}Eu_x(PO_4)_2$ were synthesized by solid-state reaction method, and their photo-luminescent properties were investigated under UV light excitation. The excitation spectra of $Na_3Gd_{1-x}Eu_x(PO_4)_2$ ($x>0$) consist a strong quasi-broad band at 370–410 nm, corresponding to the transitions $^7F_0 \rightarrow {}^5L_{6,7}$, ^5G_J. The emission spectra consist of two strong bold lines at about 594 and 618 nm, corresponding to the MD transition $^5D_0 \rightarrow {}^7F_1$ and the forced ED transition $^5D_0 \rightarrow {}^7F_2$. In our prepared samples $Na_3Gd_{1-x}Eu_x(PO_4)_2$ ($x>0$), the energy ratio (i.e., MD/ED) is 1.1, and exhibit intense reddish orange emission. The CIE chromaticity coordinates were calculated to be ($x=0.62, y=0.38$), which are close to the NTSC standard values ($x=0.67$, $y=0.33$). Efficient energy transfer from Gd^{3+} to Eu^{3+} ions has been evidenced by the excitation and emission spectra. The results indicate that the phosphor $Na_3Gd_{0.05}Eu_{0.95}(PO_4)_2$ might find a possible application on NUV InGaN chip-based WLEDs.

Acknowledgements

This work is supported by the National Natural Science Foundation of China (Nos. 21071034, 20871033).

References

[1] S. Pimputkar, J.S. Speck, S.P. DenBaars, S. Nakamura, Nat. Photon 3 (2009) 180.
[2] S. Ye, F. Xiao, Y.X. Pan, Y.Y. Ma, Q.Y. Zhang, Mater. Sci. Eng. R71 (2010) 1.
[3] D.A. Steigerwald, J.C. Bhat, D. Collins, R.M. Fletcher, M.O. Holcomb, M.J. Ludowise, P.S. Martin, S.L. Rudaz, IEEE J. Sel. Top. Quant. 8 (2002) 310.
[4] C. Guo, Y. Xu, X. Ding, M. Li, J. Yu, Z. Ren, J. Bai, J. Alloys Compd. 509 (2011) L38.
[5] R. Praveena, L. Shi, K.H. Jang, V. Venkatramu, C.K. Jayasankar, H.J. Seo, J. Alloys Compd. 509 (2011) 859.
[6] K. Shioi, Y. Michiue, N. Hirosaki, R. Xie, T. Takeda, Y. Matsushita, M. Tanaka, Y.Q. Li, J. Alloys Compd. 509 (2011) 332.
[7] J.K. Sheu, S.J. Chang, C.H. Kuo, Y.K. Su, L.W. Wu, Y.C. Lin, W.C. Lai, J.M. Tsai, G.C. Chi, R.K. Wu, IEEE Photon. Tech. Lett. 15 (2003) 18.
[8] P. Schlotter, J. Baur, Ch. Hielscher, M. Kunzer, H. Obloh, R. Schmidt, J. Schneider, Mater. Sci. Eng. B 59 (1999) 390.
[9] T. Tamura, T. Setomoto, T. Taguchi, J. Lumin. 87–89 (2000) 1180.
[10] T. Jüstel, in: C. Ronda (Ed.), Luminescence, Wiley-VCH, Weinheim, 2004, p. 184.
[11] X.P. Chen, F. Xiao, S. Ye, X.Y. Huang, G.P. Dong, Q.Y. Zhang, J. Alloys Compd. 509 (2011) 1355.
[12] M.G. Brik, Y.X. Pan, G.K. Liu, J. Alloys Compd. 509 (2011) 1452.
[13] C. Shen, K. Li, Proc. SPIE 7516 (2009) 751609.
[14] X. Zhang, M. Gong, J. Alloys Compd. 509 (2011) 2850.
[15] Y. Shi, Y. Wang, Z. Yang, J. Alloys Compd. 509 (2011) 3128.
[16] Y. Gu, Q. Zhang, Y. Li, H. Wang, J. Alloys Compd. 509 (2011) L109.
[17] G. Blasse, A. Bril, C. Nieuwpoort, J. Phys. Chem. Solids 27 (1966) 1587.
[18] Joint Committee on Powder Diffraction Standards, Card 29-1208. (JCPDS, Swarthmore, Pennsylvania).
[19] R. Salmon, C. Parent, M. Vlasse, G. Le Flem, Mater. Res. Bull. 13 (1978) 439.
[20] W. Szuszkiewicz, B. Keller, M. Guzik, T. Aitasalo, J. Niittykoski, J. Hölsä, J. Legendziewicz, J. Alloys Compd. 341 (2002) 297.
[21] Z.J. Chao, C. Parent, G. Le Flem, P. Hagenmuller, J. Solid State Chem. 82 (1989) 255.

[22] L. Schwarz, M. Kloss, A. Rohmann, U. Sasum, D. Haberlandl, J. Alloys Compd. 275–277 (1998) 93.
[23] T. Aitasalo, M. Guzik, W. Szuszkiewicz, J. Hölsä, B. Keller, J. Legendziewicz, J. Alloys Compd. 380 (2004) 405.
[24] M. Guzik, T. Aitasalo, W. Szuszkiewicz, J. Hölsä, B. Keller, J. Legendziewicz, J. Alloys Compd. 380 (2004) 368.
[25] J. Legendziewicz, M. Guzik, J. Cybińska, A. Stefan, V. Lupei, J. Alloys Compd. 451 (2008) 158.
[26] J. Legendziewicz, M. Guzik, J. Cybińska, Opt. Mater. 31 (2009) 567.
[27] M. Guzik, J. Legendziewicz, W. Szuszkiewicz, A. Walasek, Opt. Mater. 29 (2007) 1225.
[28] M. Kloss, B. Finke, L. Schwarz, D. Haberland, J. Lumin. 72–74 (1997) 684.
[29] M. Guzik, J. Legendziewicz, W. Szuszkiewicz, A. Walasek, Z. Anorg. Allg. Chem. 633 (2007) 310.
[30] Y.H.-P. Hong, S.R. Chinn, Mater. Res. Bull. 11 (1976) 421.
[31] M. Toumi, L. Smiri-Dogguy, A. Bulou, Eur. J. Inorg. Chem. 1999 (1999) 1545.
[32] D. Mizer, L. Macalik, P.E. Tomaszewski, R. Lisiecki, P. Godlewska, A. Matraszek, I. Szczygieł, M. Zawadzki, J. Hanuza, J. Nanosci. Nanotechnol. 9 (2009) 5164.
[33] V.F. Kharsika, L.N. Komissarova, A.N. Kirichenko, E.N. Murav'ev, V.P. Orlovskii, A.P. Chernyaev, Inorg. Mater. 37 (2001) 963.
[34] I. Szczygieł, L. Macalik, E. Radomińska, T. Znamierowska, M. Maczka, P. Godlewska, J. Hanuza, Opt. Mater. 29 (2007) 1192.
[35] A. Matraszek, L. Macalik, I. Szczygieł, P. Godlewska, P. Solarz, J. Hanuza, J. Alloys Compd. 451 (2008) 254.
[36] V.A. Morozov, A.P. Bobylev, N.V. Gerasimova, A.N. Kirichenko, V.V. Mikhailin, G.Ya. Pushkina, B.I. Lazoryak, L.N. Komissarova, Russ. J. Inorg. Chem. 46 (2001) 711.
[37] R.D. Shannon, Acta Cryst. A 32 (1976) 751.
[38] Y. Li, Y. Chang, Y. Lin, Y. Chang, Y. Lin, J. Alloys Compd. 439 (2007) 367.
[39] I. Omkaram, B. Vengala Rao, S. Buddhudu, J. Alloys Compd. 474 (2009) 565.
[40] G. Blasse, Struct. Bond. 26 (1976) 43.
[41] W.T. Carnall, P.R. Fields, K. Rajnak, J. Chem. Phys. 49 (1968) 4412.
[42] G. Blasse, Prog. Solid State Chem. 18 (1988) 79.
[43] W. Park, C.J. Summers, Y.R. Do, H.G. Yang, J. Mater. Sci. 37 (2002) 4041.